ESC European Society of Cardiology
Europace (2021) **23**, i80–i87
doi:10.1093/europace/euaa396

SUPPLEMENT PAPER

Novel *CineECG* enables anatomical 3D localization and classification of bundle branch blocks

Machteld J. Boonstra[1], Bashar N. Hilderink[1], Emanuela T. Locati[2], Folkert W. Asselbergs [1,3,4], Peter Loh[1], and Peter M. van Dam [1,5]*

[1]Division Heart & Lungs, Department of Cardiology, University Medical Center Utrecht, Utrecht 3508 GA, Heidelberglaan 100, Utrecht, The Netherlands; [2]Department of Arrhythmology and Electrophysiology, IRCCS Policlinico San Donato, Milano, Italy; [3]Netherlands Heart Institute, Utrecht, The Netherlands; [4]Institute of Cardiovascular Science, Institute of Health Informatics, Faculty of Population Health Sciences, University College London, London, UK; and [5]ECG Excellence BV, Nieuwerbrug aan den Rijn, The Netherlands

Received 21 November 2020; editorial decision 2 December 2020; accepted after revision 3 December 2020

Aims Ventricular conduction disorders can induce arrhythmias and impair cardiac function. Bundle branch blocks (BBBs) are diagnosed by 12-lead electrocardiogram (ECG), but discrimination between BBBs and normal tracings can be challenging. *CineECG* computes the temporo-spatial trajectory of activation waveforms in a 3D heart model from 12-lead ECGs. Recently, in Brugada patients, *CineECG* has localized the terminal components of ventricular depolarization to right ventricle outflow tract (RVOT), coincident with arrhythmogenic substrate localization detected by epicardial electro-anatomical maps. This abnormality was not found in normal or right BBB (RBBB) patients. This study aimed at exploring whether *CineECG* can improve the discrimination between left BBB (LBBB)/RBBB, and incomplete RBBB (iRBBB).

Methods and results We utilized 500 12-lead ECGs from the online Physionet-XL-PTB-Diagnostic ECG Database with a certified ECG diagnosis. The mean temporo-spatial isochrone trajectory was calculated and projected into the anatomical 3D heart model. We established five *CineECG* classes: 'Normal', 'iRBBB', 'RBBB', 'LBBB', and 'Undetermined', to which each tracing was allocated. We determined the accuracy of *CineECG* classification with the gold standard diagnosis. A total of 391 ECGs were analysed (9 ECGs were excluded for noise) and 240/266 were correctly classified as 'normal', 14/17 as 'iRBBB', 55/55 as 'RBBB', 51/51 as 'LBBB', and 31 as 'undetermined'. The terminal mean temporal spatial isochrone contained most information about the BBB localization.

Conclusion *CineECG* provided the anatomical localization of different BBBs and accurately differentiated between normal, LBBB and RBBB, and iRBBB. *CineECG* may aid clinical diagnostic work-up, potentially contributing to the difficult discrimination between normal, iRBBB, and Brugada patients.

Keywords Electrocardiogram • Vectorcardiography • *CineECG* • Cardiac modelling • Ventricular conduction disorders • Mean temporal spatial isochrones

Introduction

Normal ventricular activation is mediated through the His-Purkinje system, which rapidly distributes the electrical depolarization wave to the left ventricular (LV) and right ventricular (RV) endocardium.[1–4] The His-bundle system originates at the AV-node and directly divides into several major branches. These major branches divide numerously and terminate in a dense distribution of Purkinje fibres, distributed in a large part of the ventricular endocardium. Conduction defects in one (or more) of these mayor branches regionally delay activation. Ventricular conduction disorders may induce arrhythmias[5] and may impair cardiac function, due to the asynchronous ventricular

* Corresponding author. Tel: +31 622 198 396, *E-mail address*: peter.van.dam@peacs.nl

What's new?

- *CineECG* provided an automatic and quantitative differentiation between conduction defects by relating ventricular activation to cardiac anatomy of a standard a 3D heart model.
- *CineECG* provided the anatomical localization of different conduction defects and proved to be a robust method which accurately differentiated between normal, left bundle branch block and right bundle branch block, and incomplete right bundle branch block (iRBBB) electrocardiogram tracings.
- The terminal part of the mean temporal spatial isochrone trajectory contains most information about the distinct BBB anatomical localization and may specifically contribute to the identification of iRBBB.

activation.[6,7] Intra-ventricular conduction disorders are typically referred to as bundle branch blocks (BBBs) and are currently identified using the standard 12-lead electrocardiogram (ECG).

The diagnostic value of the standard 12-lead ECG is limited by the difficulty of linking the ECG data directly to cardiac anatomy. Furthermore, mechanical noise, and inconsistency and variability in electrode positioning may significantly influence recorded ECG waveforms, thereby directly affecting ECG interpretation.[8–10] These factors may contribute to the challenges of the discrimination between BBB and normal tracings. For many decades, the vectorcardiogram (VCG) was thought to overcome these issues as it represents the direction of cardiac activity, either depolarization or repolarization.[11] However, the relation between the VCG and cardiac anatomy remains complex. Therefore, the identification of BBB using the 12-lead ECG remains cumbersome, even for expert ECG-readers.

Complete and incomplete BBB are identified by specific 12-lead ECG waveform characteristics. However, incomplete BBBs may be difficult to detect as the late activated area is relatively small resulting in subtle ECG waveform changes.[12] Moreover, while in the past, incomplete right bundle branch block (iRBBB) and right bundle branch block (RBBB) were typically thought to be benign findings in young adults, more recent studies suggest that they may be associated with severe disease, in both symptomatic and asymptomatic patients.[13] Thus, patients found to have such abnormalities should undergo careful examination to exclude cardiac disease. Furthermore, iRBBB waveform characteristics may resemble non-diagnostic waveform abnormalities detected in patients with suspect Brugada syndrome (BrS), referred to as Type 2 or 3 BrS patterns. Often, even expert cardiologists do not agree on ECG interpretations of BrS patterns, providing inconsistent and discordant diagnostic conclusions.[14] Therefore, the correct identification of iRBBB, is of major clinical relevance.

The *CineECG* method, computes the mean temporo-spatial isochrone (mTSI) trajectory of ECG waveforms and projects this into a 3D heart model, thereby representing the mean trajectory of the ventricular electrical activation at any time interval related to ventricular anatomy.[15,16] Recently, in Brugada patients, both with spontaneous or with Ajmaline-induced Type 1 pattern, *CineECG* has localized the terminal components of ventricular depolarization to the right ventricle outflow tract (RVOT). This localization coincided with the anatomical arrhythmogenic substrate location detected by epicardial potential–duration maps. This abnormality was not found in normal subjects or in RBBB patients. *CineECG* may be a useful tool to more accurately identify conduction disorders in specific areas of the heart, such as LV, septum, or RV, overcoming the challenges of the standard 12-lead ECG interpretation.

This study aimed at exploring whether abnormalities of the mTSI trajectory computed by *CineECG* can allow a simple and precise identification of bundle branch conduction defects, thereby providing a more objective and reproducible discrimination between normal, left BBB (LBBB), RBBB, and iRBBB compared with the standard interpretation of the 12-lead ECG.

Methods

CineECG method

CineECG relates electrical cardiac activity to cardiac anatomy by computing the mTSI trajectory. In summary, the mTSI trajectory is derived from the VCG, computed from 12-lead ECG while taking into account the electrode positions on the thorax. Subsequently, a constant conduction velocity is used to project the location of the mTSI trajectory per time interval inside the heart model (Supplementary material online, Methods).[17] The mTSI trajectory thus describes the mean direction of all simultaneous ventricular electrical activity during the activation and recovery of the heart, where cardiac activation is related to cardiac anatomy (*Figure 1*).[15,17] In this study, the MRI-based heart/torso anatomical model of a 58-year-old male with standard electrode positions was used in all cases.[17] The mTSI was computed according to the standard *CineECG* method.[15,17] The origin of the mTSI trajectory is located in the LV septum.[18]

The root mean square (RMS) curve from all recorded ECG leads was used to identify the onset and end of ventricular activation. Two fiducial points are identified: QRS onset (*Figure 1*, white line) and QRS end (*Figure 1*, red line). The mTSI trajectories were displayed by the standard four-chamber view, the right and left anterior oblique views (*Figure 2*).[18] This enables the quantification of the relation between cardiac anatomy and the mTSI. Establishing the relation between the cardiac anatomy and the (terminal) direction of the mTSI, allows depiction of the region of latest activation during depolarization.

Per recording, one template beat was selected and semi-automatically QRS onset and QRS end were determined (*Figure 1*, left panel). Then, up to eight eligible beats were automatically selected based on similarity of the QRS complex to the template beat (QRS correlation >0.99 and relative difference <0.15). For all selected beats, the mTSI trajectory was computed.

Electrocardiogram data and validation of the database

A total of 500 EGCs were utilized from the certified classified Physionet XL PTB Diagnostic ECG Database (500 Hz, https://physionet.org/content/ptb-xl/1.0.1/, *Table 1*). To comply with the *CineECG* data structure, signals were resampled to 1000 Hz using linear interpolation. ECGs were classified as either no conduction disturbances (normal), iRBBB, complete right bundle branch block (RBBB), complete left bundle branch block (LBBB), or other conduction disturbances. ECGs with other conduction disturbances [e.g. left anterior fascicular block (LAFB), left posterior fascicular block (LPFB), unspecified intra-ventricular conduction disturbance (IVCD), or bifascicular blocks] were excluded from analysis.

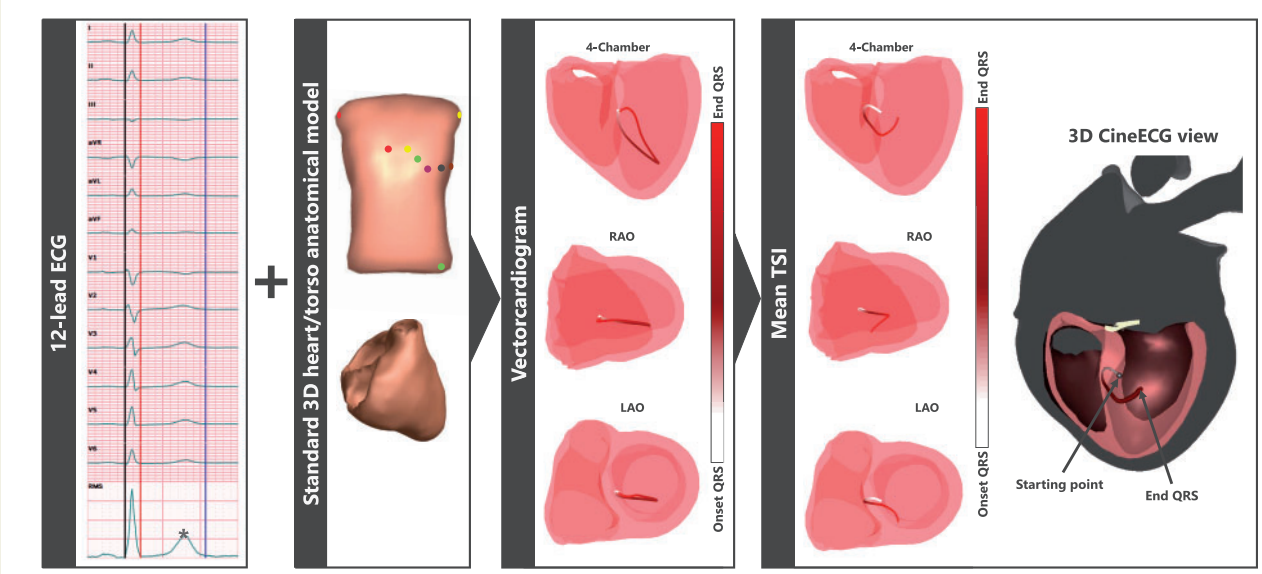

Figure 1 The computation of the mTSI trajectory. First, the standard 12-lead ECG (left box) is used to compute the vectorcardiogram. Subsequently the mTSI locations are computed with starting point at the centre of the ventricular mass projected into the LV septum (right box, arrow starting point) by taking into account electrode positions and the anatomical location of the heart. The mTSI trajectory is constructed as the 3D location of activation per millisecond moving with a velocity of 0.7 m/s. The QRS complex is segmented using the white and red line. These colours correspond to the colours in the vectorcardiogram and mTSI trajectory, which is displayed in 2D view and 3D view (3D *CineECG* view). Trajectories are either displayed in the four-chamber view (4-chamber), the LAO view, the RAO view, or the AP view. AP, anterior–posterior; ECG, electrocardiogram; LAO, left anterior oblique; LV, left ventricular; mTSI, mean temporal spatial isochrone; RAO, right anterior oblique.

Due to inconsistencies in the PTB database classification observed prior to the *CineECG* analysis, two trained experts (B.N.H. and M.J.B.) independently re-evaluated all ECG classifications according to the AHA Guidelines.[19] The classifications of B.N.H. and M.J.B. were combined, inconsistencies identified and consensus was reached from a definitive classification. Compared with the PTB database-classification, a total of 151 ECGs were reclassified. A total of 109 ECGs were excluded from analysis as those were classified as either noise, LAFB, LPFB, IVCD, or bifasicular blocks. The definitive classification was used as gold standard.

CineECG parameters

For all 2993 beats from the included 391 ECGs, the following *CineECG* parameters were computed to describe the mTSI trajectory:

Three-dimensional area

The 3D mTSI area is defined as the area encapsulated by the mTSI trajectory. The QRS area is defined as the area under the *X*, *Y*, and *Z* leads which are used to compute the VCG.[20]

Mean temporal spatial isochrone location

For each mTSI 1 ms time interval, the mTSI location is determined; e.g. inside the septum, the LV, or the RV. The initial (first 25 ms), average, and terminal (last 25 ms) locations of the mTSI are determined. Each time interval location is labelled to one of the designated areas and displayed as the ratio per area class. During normal activation, a trans-septal activation wavefront is expected to be present as activation is first initiated at the LV septum and then moves towards the RV. If the initial trajectory is located >10 ms inside the septum, a trans-septal initial vector is classified as present.

Mean temporal spatial isochrone direction

The main direction is identified as the ratio of activation directed from anterior to posterior, right to left, or apex to base with respect to the cardiac anatomy, different from the traditional azimuth, and elevation known from VCG analysis which are referenced to the thorax. This ratio is calculated by determining per time interval the direction of the mTSI trajectory. A positive direction indicates movement towards the posterior, left, or basal area, respectively. A value of zero indicates no movement towards the denoted area. The more positive or negative the value; the more the mTSI trajectory moves towards, respectively, away from the area. The initial (first 25 ms), average and terminal (last 25 ms) mTSI trajectory direction was determined.

Trans-cardiac ratio

The trans-cardiac ratio (TCR) is the ratio of the 3D distance between the location of QRS onset and QRS end and heart-model size.[16] The minimal TCR is the ratio of the 3D distance between the location of QRS onset and the closest point of the mTSI trajectory to the onset after 60% of the QRS duration and heart-model size.

Heart axis

A frontal and transversal heart axis were defined by calculating the angle between the left to right axis and a predefined location in the mTSI trajectory. An initial (25 ms), average, and terminal (QRS end) location in the mTSI trajectory were computed.

CineECG classification

Relevant *CineECG* parameter and cut-offs were identified using scatter plots, where the relevant parameter (*y*-axis) was scattered against QRS duration (*x*-axis). Based on this analysis and a previous study, all beats were classified using the *CineECG* parameters using the following criteria[17]:

(1) Normal: QRS duration < 110 ms, TCR 2–40%, terminal-mTSI location RV < 50%, and the terminal transversal heart axis between −100° and 150°.
(2) RBBB: QRS duration ≥ 120 ms, TCR > 8%, terminal-mTSI location RV, or septum > 0. Terminal transversal heart axis <−50° or >50°.
(3) iRBBB QRS duration ≥100 and < 120 ms, minimal TCR < 15%, mTSI location in RV. Terminal transversal heart axis <−75° or >75°.
(4) LBBB: QRS duration ≥120 ms, TCR > 35%, average transversal HA terminal QRS between 0 and 100, complete mTSI location >70% inside the LV.
(5) Undetermined: any other value for the above-mentioned *CineECG* parameters.

If in a given ECG, different beats were allocated to different *CineECG* classes, the final *CineECG* class of the complete ECG was determined by identifying the most frequently assigned *CineECG* class over all considered beats.

Statistical analysis

All statistical analysis was performed using MATLAB (2017a). The percentage of correctly classified ECGs was determined as well as sensitivity, specificity, negative predictive value, positive predictive value, accuracy, and F1-score were determined per subgroup. Baseline characteristics were tested for statistically significant difference using one-way ANOVA or χ^2 tests for continuous, respectively, categorical variables. A value of $P < 0.05$ was considered statistically significant.

Results

The clinical, ECG, and *CineECG* characteristics of the 391 cases grouped by their clinical diagnosis are provided in *Table 1*. As can be observed, the age between clinical groups differed significantly ($P < 0.0001$). Furthermore, all *CineECG*-derived parameters differed significantly per group ($P < 0.0001$).

Mean temporal spatial isochrone trajectory by each clinical group

The average mTSI trajectories from all 2993 beats per clinical group are shown in *Figure 2*. Per time interval, the average mTSI location was computed (*Figure 2*, solid red line) and the standard deviation was calculated as the mean 3D distance between the average mTSI trajectory and individual mTSI trajectories (*Figure 2*, grey tubular envelope). A clear distinction between normal, RBBB, and LBBB activation can be observed. In RBBB activation, the initial part of the mTSI is similar to normal activation whereas in LBBB activation the initial trans-septal direction is not present. Differences between iRBBB and normal activation are less pronounced compared with the complete blocks.

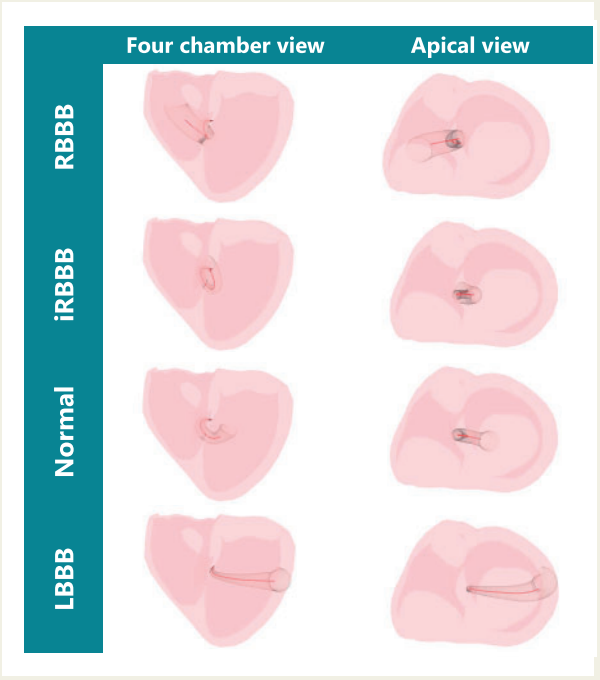

Figure 2 The average *CineECG* mTSI trajectories according to ECG diagnosis. For all four groups: normal, iRBBB, RBBB, and LBBB, mTSI trajectories are displayed in the four-chamber view (left column) and apical view (right column). The standard deviation around the average mTSI trajectory is indicated by the black tubular envelope and the mean mTSI direction is indicated in red. ECG, electrocardiogram; iRBBB, incomplete right bundle branch block; LBBB, left bundle branch block; mTSI, mean temporal spatial isochrone; RBBB, right bundle branch block.

Normal activation

In the 266 cases defined on the basis of the 12-lead ECG classification as normal, the mTSI trajectory was compact (*Figure 2*). The initial direction of the mTSI trajectory was mainly trans-septal, crossing the septal wall from left to right (*Table 1*). Thereafter, the main direction was towards the middle/basal area of the LV-free wall. Overall, the mTSI of the QRS stayed close to or inside the septum and terminated in the LV.

Incomplete bundle branch block activation

In the 17 cases defined as iRBBB, the mTSI trajectory was even more compact compared with the normal mTSI trajectory (*Figure 2*). The first part of the mTSI trajectory is similar to the normal mTSI trajectory. After the initial trans-septal movement, the mTSI starts moving towards the apex and back through the septal wall towards the LV. The terminal part points mostly towards the septal wall, indicating late activation in the RV. This compactness was reflected in a lower TCR and minimal TCR and the mTSI location was high for the septum.

Table 1 The clinical, electrocardiographic, and *CineECG* characteristics of the 391 cases grouped by their clinical diagnosis

	Normal	iRBBB	RBBB	LBBB	*P*
Clinical characteristics					
Cases, *n*	266	17	55	51	
Beats, *n*	2065	126	409	393	
Age (years)	47 ± 19	47 ± 20	69 ± 14	74 ± 9	<0.0001
Gender (% male)	54	35	42	59	0.132
CineECG characteristics					
QRS duration (ms)	87 ± 10	108 ± 5	141 ± 13	144 ± 14	<0.0001
QT duration (ms)	395 ± 34	411 ± 42	439 ± 58	431 ± 54	<0.0001
TCR (%)	21 ± 9	18 ± 8	41 ± 9	48 ± 4	<0.0001
Minimal TCR (%)	18 ± 10	11 ± 9	21 ± 15	48 ± 4	<0.0001
Trans-septal vector present (%)	95	97	87	47	<0.0001
Angle trans-septal initial vector (%)	129 ± 28	134 ± 23	123 ± 30	82 ± 37	<0.0001

Values are displayed as mean ± standard deviation, a *P*-value <0.05 was considered statistically significant.
iRBBB, incomplete right bundle branch block; LBBB, left bundle branch block; QRS, QRS complex; QT, Q-wave to end T-wave; RBBB, right bundle branch block; TCR, trans cardiac ratio.

Right bundle branch block activation

In the 55 cases defined as RBBB, the mTSI trajectory differed from the normal mTSI trajectory in its terminal QRS direction which was directed towards the right basal area (*Figure 2*), reflecting late ventricular activation in this region. Compared with normal TCR, the TCR was increased and increased mTSI location inside the RV was observed. The trans-septal vector was less present compared with normal and iRBBB mTSI trajectories (*Table 1*).

Left bundle branch block activation

In the majority of the 51 cases defined as LBBB, a trans-septal vector was absent in the mTSI trajectory. In these subjects, the mTSI moved from the LV septal wall towards the LV-free wall, which was reflected in the mTSI location. The terminal mTSI of the QRS was directed to the LV-free wall (b), with a large TCR (*Table 1*), the mTSI was never located in the RV, and a trans-septal vector was less present (*Table 1*).

CineECG classification output

All 2993 beats (from 391 ECGs) were classified according to the *CineECG* criteria as either 'normal', 'iRBBB', 'RBBB', 'LBBB', or 'undetermined', and these classifications were used to determine the definitive *CineECG* class per ECG. Two-dimensional scatterplots were used to determine the relevancy and cut-off values per *CineECG* parameter (*Figure 3A*). In 41 ECGs, beats of one ECG were assigned to two or more CineECG classes, either to the 'normal', 'iRBBB', or 'undetermined' group and thereof 27 ECGs were classified correctly. *Table 2* shows the detailed diagnostic performance of the *CineECG* classification for the different clinical groups. A high performance was obtained for normal, RBBB, and LBBB groups. For iRBBB activation, sensitivity was lower compared with the other groups. For RBBB and LBBB groups, the *CineECG* classification and the clinical diagnosis were always coincident (*Figure 3B*). Vice versa, less consistency between *CineECG* and clinical diagnosis was observed in discriminating between iRBBB from normal, especially in beats with a QRS duration between 100 and 110 ms.

Discussion

This is the first study utilizing *CineECG* to characterize ventricular activation defects and classify BBB by using 3D anatomical characteristics of the mTSI trajectory. Using *CineECG* criteria, all RBBB and LBBB tracings, and most IRBB and normal tracings, were classified correctly in accordance with standard 12-lead clinical classification. *CineECG* provides an easy to use tool to obtain a comprehensive insight into the relation between ventricular activation and anatomy and is therefore helpful for clinicians to accurately discriminate between different conduction disorders. However, between iRBBB and normal activation, overlap exists between the clinical groups, particularly between 100 and 120 ms QRS duration. A clear distinction between the types of blocks can be visually observed in the average mTSI trajectories (*Figure 2*). The terminal vector of the mTSI trajectory points towards the area of latest activation, thereby indicating the location of the block. However, the differentiation between an iRBBB and a normal pattern remains challenging and requires further optimization.

The relation between mean temporal spatial isochrone and bundle branch block location

The average mTSI trajectories observed in this study, clearly show distinct patterns for different types of BBB (*Figure 2*). For the complete BBB, a clearly deviating pattern from the normal can be observed. While in LBBB activation patterns, the mTSI trajectory mainly moves leftwards and inside the LV cavity, in RBBB activation patterns, the mTSI trajectory initially moves towards the LV cavity whereafter it moves towards the RV basal area (*Figure 2*). Thus, while the mTSI trajectory of LBBB solely moves leftwards, the mTSI trajectory for

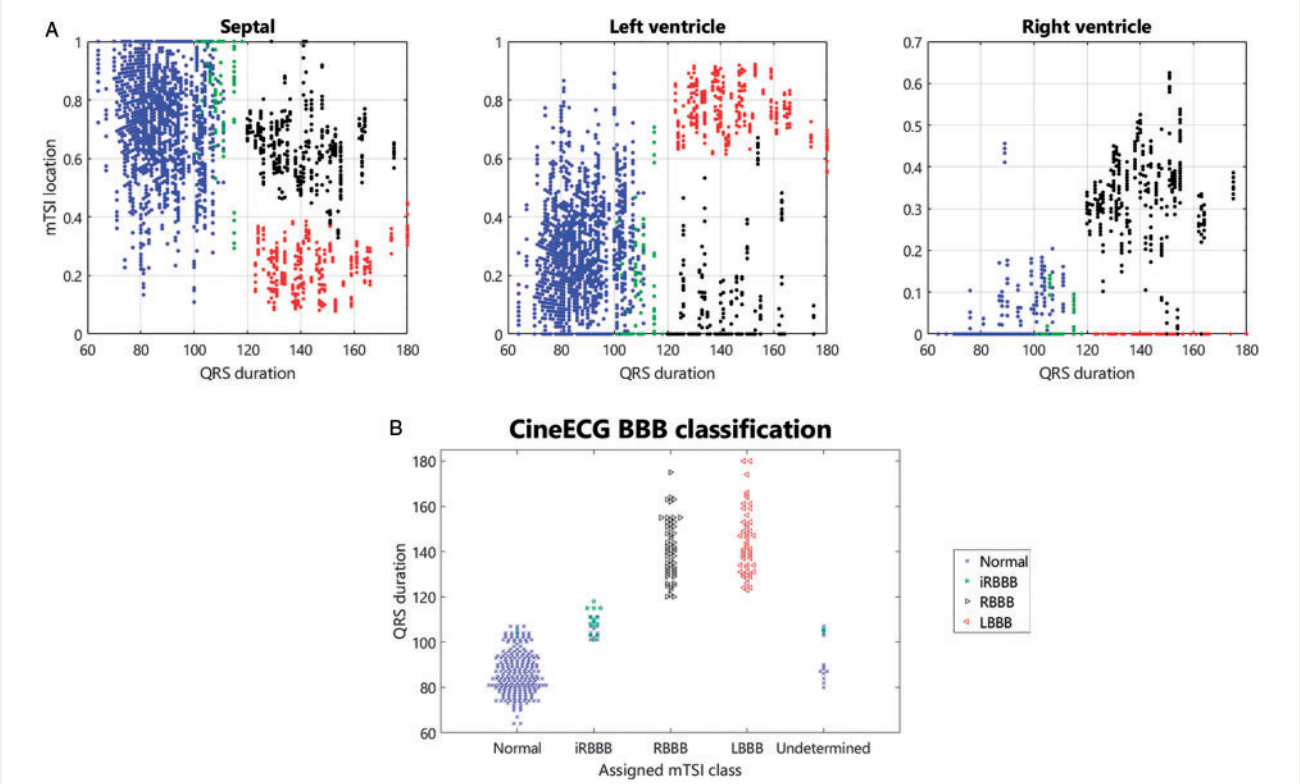

Figure 3 (*A*) The *CineECG* BBB classification criteria were based on 2D scatterplots of various *CineECG* parameters. A representative example of the scatterplot of the mTSI area class parameter against QRS duration (*x*-axis) is shown. These scatterplots were used to identify the relevancy and cut-off values of *CineECG* parameters. The final *CineECG* criteria were set by a combination of data obtained in a previous study[17] and observations made in the current study. (*B*) *CineECG* BBB classification. The beat adjudication according to the *CineECG* criteria (*x*-axis) against QRS duration (*y*-axis) to show overlap between QRS duration but were assignment to a different group. Colours of the dots indicate the clinical group. The dots in all plots indicate measured values per beat plotted as a function of QRS duration, diagnosed as either normal (blue), RBBB (black), iRBBB (green), or LBBB (red). iRBBB, incomplete right bundle branch block; LBBB, left bundle branch block; mTSI, mean temporal spatial isochrone; RBBB, right bundle branch block.

Table 2 The overall performance of the *CineECG* classification scheme for the classification of ECGs

	Normal	iRBBB	RBBB	LBBB
Sensitivity	90.2	82.4	100	100
Specificity	99.2	96.5	100	100
Negative predictive value	82.4	99.2	100	100
Positive predictive value	99.6	51.9	100	100
Accuracy	94.7	63.6	100	100
F1-score	93.1	95.9	100	100

Values are displayed as percentages. Ranges of confidence intervals were equal to the mean presented in this table.
ECG, electrocardiogram; iRBBB, incomplete right bundle branch block; LBBB, left bundle branch block; RBBB, right bundle branch block.

RBBB starts leftwards, and then goes rightwards. This may be explained by the larger amount of LV myocardial mass, with respect to the RV myocardial mass, and thus LV activation is likely to conceal activation occurring in the RV. Since *CineECG* takes cardiac anatomy into account, mTSI trajectories might be viewed as a more reliable alternative to identifying BBB than the current ECG strict criteria for LBBB and RBBB, also considering inter-individual age and gender variation.[6,12]

Clinical classification of incomplete right bundle branch block

QRS duration is one of the main clinical characteristics to differentiate between normal, incomplete, and complete RBBB. An iRBBB is identified when QRS-duration ranges between 110 and 120 ms, but may be wrongly classified in cases of incorrect manual or machine interpretation of the 12-lead ECG, further magnified due to inter-lead QRS duration differences. Therefore, a coherent way to measure the QRS duration is of utmost importance in order to correctly differentiate between normal and iRBBB activation. *CineECG* is likely to overcome these difficulties. In case of iRBBB, the mTSI trajectory is compact and stays within the septum and clearly differs from both normal and RBBB activation (*Figure 2*). Thus, (i) the temporo-spatial location of the mTSI trajectory contains all information about the direction and timing of ventricular depolarization and (ii) the mTSI

terminal direction indicates the anatomical location of the block, by pointing towards the latest site of activation. With increasing QRS duration in iRBBB cases, a clear shift of the terminal mTSI direction towards the RV base was observed, becoming more similar to the RBBB mTSI trajectory (*Figure 2*).

Comparison with standard 12-lead electrocardiogram assessment

In this study, we validated our *CineECG* method with the clinical 12-lead ECG assessment. However, ultimately, the comparison of *CineECG* classification with standard 12-lead ECG clinical assessment through invasive electro-anatomical activation mapping should be performed. Through invasive mapping, the true location of the BBB may be identified and the ability of *CineECG* and standard clinical 12-lead to identify these BBBs correctly can then be assessed.

Starting point mean temporal spatial isochrone trajectory

In *CineECG*, the starting point of the mTSI trajectory was set at the left side of the septal wall closest to the ventricular centre of mass. During normal activation, a trans-septal wavefront of activation moves from the LV side of the septum towards the right. However, in LBBB cases the trans-septal vector is reversed and thus classified as not present in 53% (*Table 1*). Therefore, this starting point may inadequately represent the true start of LBBB activation, as such activation starts at the RV septum or RV-free wall. Furthermore, due to intra-individual differences in bundle branch anatomy, this starting point may inadequately represent the true starting point of ventricular activation. The starting point therefore serves as a general starting point, but as shown in this study, *CineECG* provides an accurate concise way to assess average ventricular activation related into cardiac anatomy, where the starting point does not yet seem to be a constraint for the *CineECG* classification.

Limitations

The use of a standardized heart torso model, rather than a personalized model, may limit the accuracy of the presented results. The use of the standard torso/heart model enables the direct projection of the mTSI to the cardiac anatomy, but differences in heart anatomy and orientation, thorax anatomy and lead position are not accounted for. With age, the shape, position, and orientation of the heart in the torso may change. In this study, we used a standard anatomical heart/torso model based on a 58-year-old male, which may adequately represent adult RBBB and LBBB male cases (*Table 1*) but may be inadequate for the younger iRBBB and normal cases and more generally, for female cases. Using a standardized heart/torso model may result in a larger *CineECG* parameter variation, caused by intra-individual variation in cardiac anatomy. Thus, the distribution of mTSI-derived parameters per BBB group encompass larger standard deviations as activation is referenced to a cardiac anatomy with an incorrect size, shape, and/or orientation, also relative to the thoracic model and electrode locations. Therefore, using a 3D camera to localize the ECG electrodes and the torso dimensions might increase the accuracy of our method.[21–23] These factors may be particularly relevant for the more accurate identification of iRBBB.

In PTB database, the number of IRBB cases was very small. Besides, we found some inconsistencies in the PTB database classification, particularly regarding iRBBB cases. Therefore, we revised all the included ECG and upon agreement of two independent experts, we came to a definitive classification of the PTB tracings which we used for the statistical analysis. Given the clinical relevance of analysis of the late depolarization signals, we plan to perform a prospective study studying *CineECG* characteristics of patients with different intra-ventricular conduction disorders.

Future perspectives

Ambiguity in the standard 12-lead ECG classification can be caused by the presence of intra-individual differences in cardiac anatomy (size, shape), cardiac orientation (due to age, effects of breathing, thoracic shape), bundle branch anatomy, the presence of cardiac disease (scar, myocarditis, fibrofatty tissue), and inconsistency in the placement of electrodes relative to the heart. All these factors may contribute to determine the ECG waveform morphology and 12-lead ECG diagnostic criteria of BBB may be present in the 12-lead ECG in the absence of a true BBB. Through *CineECG*, a more comprehensive view is given on the cardiac electrical activity using the 12-lead ECG, thereby providing a tool less prone to intra-individual characteristics. Further testing and optimization of this technique are still required. For example, the effect of the presence of scar or ischaemia, or more generally myocardial structural diseases, should be assessed in future studies. Furthermore, the ability of *CineECG* to correctly discriminate between iRBBB, RBBB, LBBB, unspecified intra-ventricular conduction disorders and left anterior and posterior hemiblocks, or even the coexistence of these conduction disturbances should be assessed.

Conclusions

The advanced interpretation of the 12-lead ECG through the *CineECG* method proved to be a robust technique to differentiate between different intra-ventricular bundle branch conduction defects. The mTSI trajectory relates cardiac activation to cardiac anatomy, thereby directly identifying the anatomical location of the BBB, mostly indicated by the terminal part of the mTSI trajectory. The *CineECG* classification was able to accurately discriminate between normal, RBBB, and LBBB cases. Further optimization of the classification algorithm may enhance the *CineECG* classification of iRBBB. The *CineECG* method, directly derived from 12-lead ECG, can be viewed as a non-invasive mapping tool and may improve the early recognition and the monitoring of the progression of intra-ventricular bundle branch conduction defects.

Supplementary material

Supplementary material is available at *Europace* online.

Acknowledgements

We would like to thank Judith van Oosterom for her proof reading of our manuscript. This work would not have been possible without the foundation provided by Adriaan van Oosterom. We keep you in our hearts!

Funding

This work was supported by the Netherlands Cardiovascular Research Initiative, an initiative with support of the Dutch Heart Foundation (grant number QRS-Vision 2018B007). F.W.A. was supported by UCL Hospitals NIHR Biomedical Research Centre. This paper is part of a supplement supported by an unrestricted grant from the Theo-Rossi di Montelera (TRM) foundation.

Conflict of interest: P.M.D. is one of the owners of ECG Excellence.

Data availability

The data used in this manuscript are freely available from the PTB-XL Physionet database.

References

1. Tawara S. Das Reizleitungssystem des Säugetierherzens. In *Eine Anatomisch-Histologische Studie Über das Atrioventrikularbündel und die Purkinjeschen Faden*. Jena, Germany: Gustav Fischer; 1906.
2. Tawara S. Die Topographie und Histologie der Bruckenfasern. Ein Beitrag zur Lehre von der Bedeutung der Purkinjeschen faden. *Zentralb Physiol* 1906;**19**:70–6.
3. Demoulin J, Kulbertus H. Histopathological examination of concept of left hemiblock. *Br Heart J* 1972;**34**:807–14.
4. Oosthoek PW, Viragh S, Lamers WH, Moorman AF. Immunohistochemical delineation of the conduction system. II: the atrioventricular node and Purkinje fibers. *Circ Res* 1993;**73**:482–91.
5. Kusumoto FM, Schoenfeld MH, Barrett C, Edgerton JR, Ellenbogen KA, Gold MR *et al.* 2018 ACC/AHA/HRS guideline on the evaluation and management of patients with bradycardia and cardiac conduction delay: a report of the American College of Cardiology/American Heart Association Task Force on Clinical Practice Guidelines and the Heart Rhythm Society. *Circulation* 2019;**140**:e382–e482.
6. Strauss DG, Selvester RH, Wagner GS. Defining left bundle branch block in the era of cardiac resynchronization therapy. *Am J Cardiol* 2011;**107**:927–34.
7. Vassallo JA, Cassidy DM, Marchlinski FE, Buxton AE, Waxman HL, Doherty JU *et al.* Endocardial activation of left bundle branch block. *Circulation* 1984;**69**:914–23.
8. Drew BJ, Adams MG. Clinical consequences of ST-segment changes caused by body position mimicking transient myocardial ischemia: hazards of ST-segment monitoring? *J Electrocardiol* 2001;**34**:261–4.
9. Macfarlane PW, Colaco R, Stevens K, Reay P, Beckett C, Aitchison T. Precordial electrode placement in women. *Neth Heart J* 2003;**11**:118–22.
10. Bond RR, Finlay DD, Nugent CD, Breen C, Guldenring D, Daly MJ. The effects of electrode misplacement on clinicians; interpretation of the standard 12-lead electrocardiogram. *Eur J Intern Med* 2012;**23**:610–5.
11. Frank E. General theory of heart-vector projection. *Circ Res* 1954;**2**:258–70.
12. Galeotti L, van Dam PM, Loring Z, Chan D, Strauss DG. Evaluating strict and conventional left bundle branch block criteria using electrocardiographic simulations. *Europace* 2013;**15**:1816–21.
13. Nasir JM, Shah A, Jones S. The significance of incomplete and complete right bundle branch blocks in young adults. *J Am Coll Cardiol* 2012;**59**:E1939.
14. Chevallier S, Forclaz A, Tenkorang J, Ahmad Y, Faouzi M, Graf D *et al.* New electrocardiographic criteria for discriminating between Brugada types 2 and 3 patterns and incomplete right bundle branch block. *J Am Coll Cardiol* 2011;**58**:2290–8.
15. van Dam PM. A new anatomical view on the vector cardiogram: the mean temporal-spatial isochrones. *J Electrocardiol* 2017;**50**:732–8.
16. Roudijk R, Loh KP, van Dam PM. Mean temporal spatial isochrones direction as marker for activation delay in patients with arrhythmogenic cardiomyopathy. *Comput Cardiol* 2018;**45**:1–4.
17. van Dam PM, Locati ET, Ciconte G, Borrelli V, Heilbron F, Santinelli V *et al.* Novel CineECG derived from standard 12-lead ECG enables right ventricle outflow tract localization of electrical substrate in patients with Brugada syndrome. *Circ Arrhythm Electrophysiol* 2020;**13**:e008524.
18. Durrer D, van Dam RT, Freud GE, Janse MJ, Meijler FL, Arzbaecher RC. Total excitation of the isolated human heart. *Circulation* 1970;**41**:899–912.
19. Surawicz B, Childers R, Deal BJ, Gettes LS. AHA/ACCF/HRS recommendations for the standardization and interpretation of the electrocardiogram: part III: intraventricular conduction disturbances: a scientific statement from the American Heart Association Electrocardiography and Arrhythmias Committee, Council on Clinical Cardiology; the American College of Cardiology Foundation; and the Heart Rhythm Society: endorsed by the International Society for Computerized Electrocardiology. *Circulation* 2009;**119**:e235–40.
20. van Stipdonk AM, Ter Horst I, Kloosterman M, Engels EB, Rienstra M, Crijns HJ *et al.* QRS area is a strong determinant of outcome in cardiac resynchronization therapy. *Circ Arrhythm Electrophysiol* 2018;**11**:e006497.
21. van Dam PM, Gordon JP, Laks M. Sensitivity of CIPS-computed PVC location to measurement errors in ECG electrode position: the need for the 3D camera. *J Electrocardiol* 2014;**47**:788–93.
22. Alioui S, Kastelein M, Em vD, Pm vD. Automatic registration of 3D camera recording to model for leads localization. *Comput Cardiol* 2017;**44**:4.
23. van Dam PM, Boyle NG, Laks MM, Tung R. Localization of premature ventricular contractions from the papillary muscles using the standard 12-lead electrocardiogram: a feasibility study using a novel cardiac isochrone positioning system. *Europace* 2016;**18**:iv16–iv22.